U.Porto Journal of Engineering, 8:6 (2022) 13-27
ISSN 2183-6493
DOI: 10.24840/2183-6493_008.006_0002

Received: 9 October, 2021
Accepted: 3 April, 2022
Published: 28 November, 2022

Raised Floor Systems with Ceramic Tiles: Resistance to Concentrated Vertical Loads

Guilherme Farias Idalêncio[1], Elídio Angioletto[2], Djeisa Pasini[3], Augusto Wanderlind[4], Jorge Henrique Piva[5], Elaine Guglielmi Pavei Antunes[6]

[1]Structural and Construction Performance Research Group, Department of Civil Engineering, University of the Southern Santa Catarina, University Avenue, 1105-University District, 88806-000 Criciúma, Santa Catarina, Brazil (guilherme.idalencio@hotmail.com) ORCID 0000-0003-3806-0351; [2]Post-graduate Programme in Materials Science and Engineering, University of the Southern Santa Catarina, University Avenue, 1105-University District, Criciúma, Santa Catarina, Brazil (ean@unesc.net) ORCID 0000-0003-4417-3440; [3]Post-graduate Programme in Materials Science and Engineering, University of the Southern Santa Catarina, University Avenue, 1105-University District, Criciúma, Santa Catarina, Brazil (djeisa.pasini@eliane.com) ORCID 0000-0001-8282-6030; [4]Structural and Construction Performance Research Group, Department of Civil Engineering, University of the Southern Santa Catarina, University Avenue, 1105-University District, 88806-000 Criciúma, Santa Catarina, Brazil (acw@unesc.net) ORCID 0000-0002-5312-9700; [5]Structural and Construction Performance Research Group, Department of Civil Engineering, University of the Southern Santa Catarina, University Avenue, 1105-University District, 88806-000 Criciúma, Santa Catarina, Brazil (jhpiva@gmail.com) ORCID 0000-0002-1753-4944; [6]Structural and Construction Performance Research Group, Department of Civil Engineering, University of the Southern Santa Catarina, University Avenue, 1105-University District, 88806-000 Criciúma, Santa Catarina, Brazil (elainegpa@unesc.net) ORCID 0000-0002-9698-1100

Abstract

The objective of this study is to evaluate the mechanical strength of raised floor systems with ceramic coatings. The raised floor prototypes are made of three types of ceramic tiles, two of which have a dimension of 60 × 60 cm and one has a dimension of 60 × 120 cm. Instrumentation is performed by attaching the strain gauges to the surface of the ceramic tiles. The raised floor prototypes are subjected to vertical compression loads until visible cracks appear on the surface of the ceramic tiles, and the resistance to system rupture is evaluated by analyzing their deformations. The results indicate that the load application position interferes with the resistive ability of the systems. Systems with plates having low water absorption and high thickness yield high breaking loads, which can be considered as the determining factors for outdoor applications of raised floor systems.

Author Keywords. Self-locking Slabs. Coating System. Strain Analysis. Fracture Mechanics.

Type: Research Article

1. Introduction

Companies in the Brazilian civil construction industry are constantly seeking to incorporate new technologies that perform well and are cost-effective because the combination of these factors contributes to the success of their business. Among the several technologies, the raised floor system is effective as it is one of the few technological innovations in the sector that provides an alternative to the traditional coating method with adhered floors (Moreiras 2014).

The raised floor systems are widely used in corporate indoors because of the functionality provided by modulation, which allows easy access to facilities such as cabling, ease of maintenance, acoustic comfort, and protection against fire (Morais et al. 2017).

The application of this system to the outdoors has several advantages. For example, the elevation of the pavement improves landscaping, stair composition, and rainwater storage. The pedestals attached to the slab act as reservoirs, which can be used for the irrigation of hanging gardens, and thus, the consumption of potable water can be reduced (Kinzel 2015).

According to the NBR 11802:1991-raised floors–specification (ABNT 2014), there are two types of raised floors—self-locking and braced structures. The self-locking structures are plates arranged in such a way to resist the horizontal and vertical loads supported on telescopic supports. In braced structures, either stringers or telescopic supports are used to support the slabs.

Commonly used raised floor systems are made of self-locking slabs of various materials supported on telescopic supports to ensure that a gap is present between the base and the finished floor. There are several types of supports available on the market in different models and they are composed of different polymers, such as polyethylene, polycarbonate, expanded polystyrene, polyvinyl chloride (PVC), and polypropylene (PP). Among these, polycarbonate is mostly used for developing supports (Moritz 2018).

Various materials, such as concrete, rock plates, wood, and ceramic, can be used to manufacture the plates that compose the raised floor system (Bernardes 2009). However, similar to conventional coatings, the mechanical performance of these materials depends on certain factors.

In the systems manufactured using polymers and ceramic tiles, thermoplastic polymers offer ductile behavior and high strain rates (Amorim 2015). Conversely, ceramic bodies are titrated as materials with little or no plastic deformation, which can characterize a brittle rupture, whose definition is based on rupture without notice (Zanotto and Migliore JR 1991).

Although there are advantages in the number of types and possibilities of use, ceramic materials have a limited capacity for plastic deformation. This mechanical characteristic makes these materials particularly sensitive to the presence of internal discontinuities, which determine the final strength of the material (Fonseca et al. 2015).

This characteristic of ceramics makes them fragile with low tenacity. This brittle nature of the materials is because of their chemical bonds (an ionic-covalent combination), which also gives the material high tensile strength (owing to the high bond strength) and low plastic strain. The mechanical behavior of these materials can be described by the fracture mechanics theory, which investigates the initiation and propagation of one or several cracks when the material is subjected to a stress field (de Albuquerque and Rodrigues 2006).

Because ceramic tiles are often used in raised floor systems, the materials' intrinsic properties should be considered as they determine their characteristics (Caccia 2012). Using these materials in external environments exposes the coatings to severe conditions owing to thermal dilatations and mechanical solicitations due to the passage of loads.

In Brazil, the lack of standards and guides of application for raised floors outdoors leads the practitioners to empiricism. Brazilian standards only consider indoor applications, where the requirements for performance and durability are quite different (Bernardes 2009). Raised floor systems are becoming more common in the world, with extensive use in many countries (Zhang, Yang, and Sidwell 2002). When one takes into consideration that the system lacks behavior and performance evaluations, the demand for research in relation to raised floor systems becomes more accentuated.

Therefore, the current study aims to evaluate, by means of deformations, the mechanical resistance of raised floor systems with the application of three different types of ceramic tiles, simulating their outdoor applications with 120 cm high pedestals.

2. Materials and Methods

2.1. Materials

The raised floor system utilized in this study was a self-locking structure made of thermoplastic polymers. Modular panels with dimensions of 60 × 60 cm and adjustable pedestals made up of modular pieces were manufactured using PP. The rigid extension tube was made of PVC. From the bottom to the top, the pedestals are first composed of the support base of the set that fits the rigid tube. The rigid tube, which had a thickness of 2 mm and provided a height adjustment that varied between 8.5 and 200 cm, was connected to the leveling screw, whose function was to perform minor height adjustments, which in turn was connected to the bushing. The bushing composes the set and supports the pedestal, whose function is to support and interlock the plates. Figure 1 presents the components of the raised floor system and system information. Figure 1(a) shows the components of the pedestal; Figure 1(b) shows the panels; Figure 1(c) illustrates the system in execution.

Figure 1: Components of the raised floor system: (a) segmented pedestal, (b) panels, (c) running system (Source: https://www.remaster.com.br)

This system had an interlocking between the components, as shown in Figure 2; Figure 2(a) shows the pedestal fixed on the panels, and Figure 2(b) shows the fitting of the pedestal on the underside of the panel.

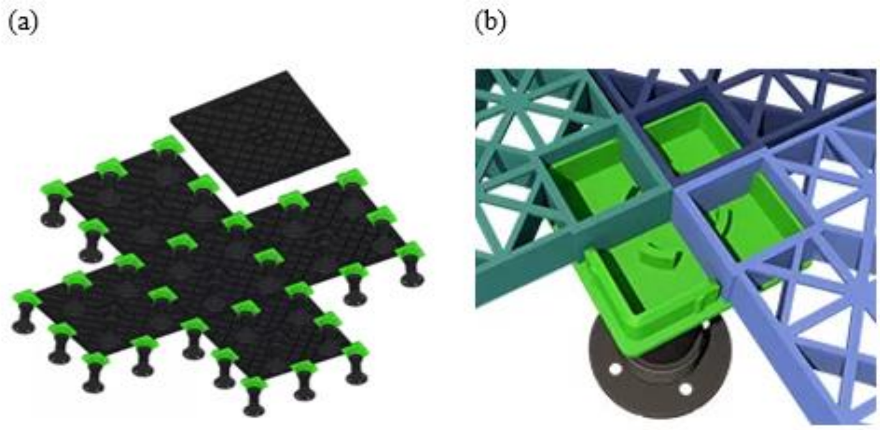

Figure 2: Interlocking the system: (a) arrangement of pedestals on panels, (b) pedestal/panel attachment (Source: https://www.remaster.com.br)

As observed in Figure 2, system interlocking was performed by fitting nine pedestals on the edges and central axis of the underside of the panel.

The top of the raised floor system consisted of ceramic tiles of three different typologies. These tiles belonged to the water absorption group BIa (0, 1–0, 5%). They were prescribed for use on indoor and outdoor floors because they exhibit low water absorption and high mechanical resistance, as presented in Table 1. Each ceramic tile typology was assigned a nomenclature based on its characteristics and dimensions. The technical porcelain tile, with dimensions of 60 × 60 cm, was named PT, the glazed porcelain tiles with dimensions of 60 × 60 cm were named PE60, and tiles with dimensions of 60 × 120 cm were named PE120.

Table 1 presents the characteristics and properties of the ceramic tiles and the nomenclature adopted for each type.

Nomenclature	PT	PE60	PE120
Ceramic tiles	Technical porcelain	Glazed porcelain	Glazed porcelain
Dimensions (cm)	60 x 60	60 x 60	60 x 120
Thickness (mm)	8,7	9,5	11
Water absorption (%)	0,1	0,5	0,5
Water absorption group	BIa	BIa	BIa
Rupture load (kN - Kgf)	1,80 - 183,55	1,50 - 152,96	2,30 - 234,53
Flexural strength module	45 - 458,87	37 - 377,29	37 - 377,29

Table 1: Ceramic tiles used (Source: From manufacturer)

2.2. Method

The three types of ceramic tiles originated from three distinct raised floor systems. The three systems were instrumented from the contact area of the load applicator (18 × 10 cm). Table 2 presents the nomenclature adopted for each system according to the ceramic tile.

Ceramic tiles	Systems	Nomenclature
PT	System with technical porcelain tiles	S-PT
PE60	System with glazed porcelain tiles 60 x 60 cm	S-PE60
PE120	System with glazed porcelain tiles 60 x 120 cm	S-PE120

Table 2: Nomenclature of the raised floor systems

From these three categories of ceramic tiles, prototypes were made with different dimensions to evaluate the load application and were instrumented with strain gauges to read the deformations in defined positions. Thus, for the S-PT and S-PE60 systems, four prototypes were created—Positions 1, 2, 3, and 4 with dimensions 60 × 60 cm, 60 × 60 cm, 60 × 120 cm, and 120 × 120 cm, respectively. For the S-PE120 system, five prototypes were produced—Positions 1.1, 1.2, 2, 3.1, and 3.2, with dimensions 60 × 120 cm, 60 × 120 cm, 60 × 120 cm, 120 × 120 cm, and 60 × 240 cm, respectively. All prototypes were mounted with 120 cm high pedestals.

2.2.1.Instrumentation

To obtain the deformation of the ceramic tiles during the application of loads in the places most susceptible to stress concentration, instrumentation of the systems was performed by gluing strain gauges to the bottom surface of the ceramic tiles. The contact area of the load applicator, positioning of the applicator, and arrangement of the strain gauges were based on the study by Medeiro (2018). The study aimed to evaluate the effect of concentrated vertical loads in a conventional flooring system covered with ceramic tiles. The center and ends of the ceramic tile were adopted to apply concentrated vertical loads and instrumentation of the system, as described by Medeiro (2018).

The S-PT and S-PE60 systems have the same instrumentation and positioning as load applicators. As shown in Figure 3, in Position 1, the center of the load applicator was aligned with the center of the ceramic tile. In Position 2, the edges of the load applicator were 5 cm from the edges of the ceramic tiles. In Position 3, the load applicator was placed over the edge of the two ceramic tiles in a centralized manner. In Position 4, the center of the load application was set at the center of four ceramic tiles over the edges.

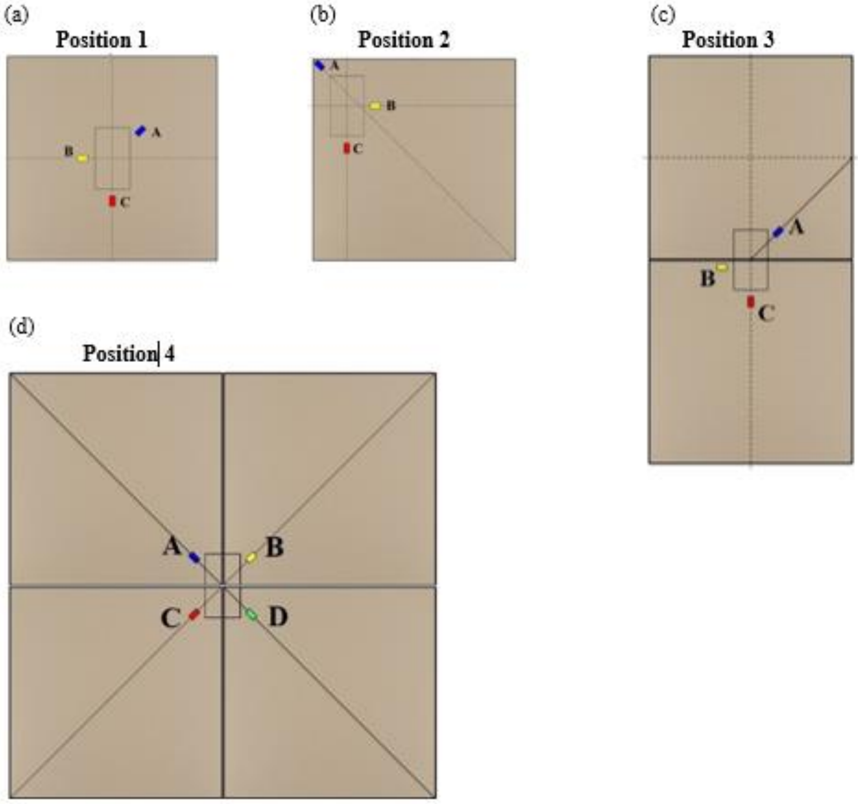

Figure 3: Systems S-PT e S-PE60: (a) Position 1, (b) Position 2, (c) Position 3, (d) Position 4

Three strain gauges named A, B, and C were fixed for Positions 1 and 2. Strain gauge A was attached tangent at 45° to the edge of the ceramic tile. Strain gauges B and C were arranged 2 cm from the load application area and aligned with the center of the load in the horizontal and vertical directions, respectively. For Position 3, the strain gauges have the exact positioning as Positions 1 and 2. Strain gauge B at Position 3 was placed 2 cm from the edge of the ceramic tile and 2 cm from the load application area. At Position 4, strain gauges A, B, C, and D were attached 45° relative to the horizontal edges of the ceramic tiles. For the S-PE120 system, the instrumentation followed the same reasoning as the S-PT and S-PE60 systems. Figure 4 shows the instrumentation of the S-PE120 system, in which the instrumentation positions at Positions 1.1, 1.2, 2, 3.1, and 3.2 are shown in Figure 4(a), Figure 4(b), Figure 4(c), Figure 4(d), and Figure 4(e), respectively.

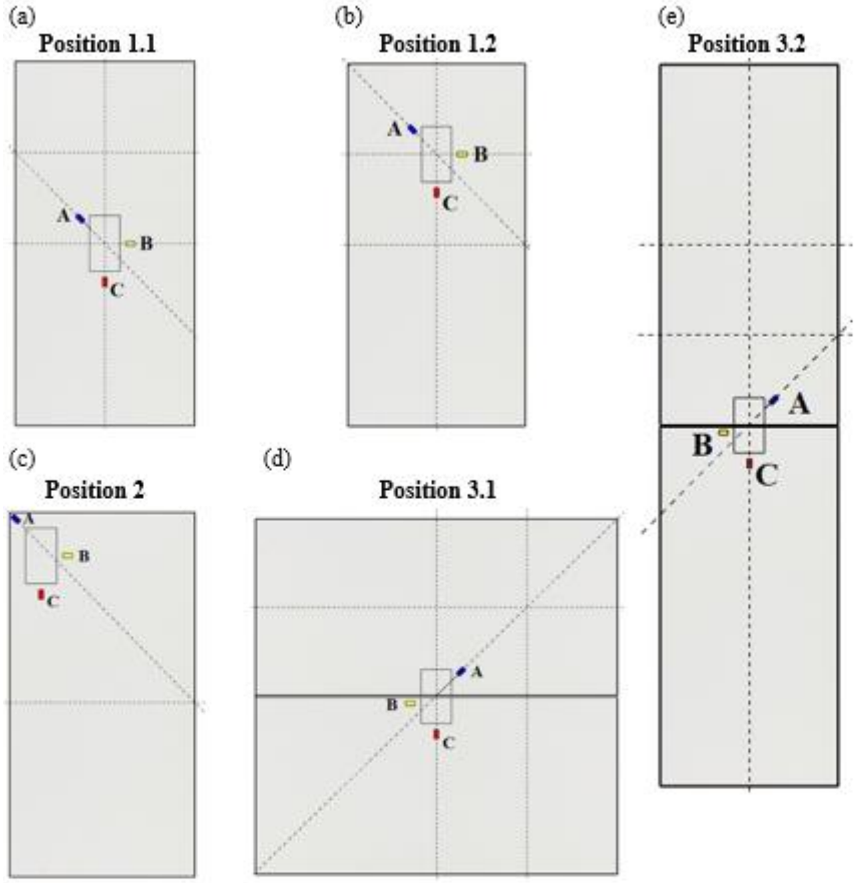

Figure 4: System S-PE120: (a) Position 1.1, (b) Position 1.2, (c) Position 2, (d) Position 3.1, (e) Position 3.2

The load applicator was positioned at five different points, the first of which was named Position 1.1, where the center of the load applicator was located at the center of a ceramic tile. In the second position (Position 1.2), the load application area was positioned at the center and top of the ceramic tile. For Position 2, the load applicator was positioned close to one end of the ceramic tile, 5 cm from the edges in the vertical and horizontal directions, as in Position 2 of the S-PT and S-PE60 systems. The last two locations of the load applicator were located between the two ceramic tiles. For Position 3.1, the load applicator was positioned between the two ceramic tiles, which had the dimensions of 60 cm. For Position 3.2, the ceramic tiles were aligned at 120 cm, and the load applicator was placed between the two tiles.

For instrumentation at Positions 1.1, 1.2, and 2 of the S-PE120 system, three strain gauges were used at each position and had the same arrangements as those at Positions 1 and 2 of the S-PT and S-PE60 systems. The strain gauges were named A, B, and C. The strain gauge A was fixed at 45° to the edge of the ceramic tile. Strain gauges B and C were arranged at 2 cm from the load application area and aligned with the center of the load in the horizontal and vertical directions, respectively.

The instrumentation of Positions 3.1 and 3.2 was performed in the same way as Position 3 of the S-PT and S-PTE60 systems. As in the instrumentation of the previous positions, three strain gauges A, B, and C, were used. For strain gauges A and C, the same position was used for Positions 1.1, 1.2, and 2. Strain gauge B was located 2 cm from the edge of the ceramic tile and 2 cm from the load-application area.

2.2.2. Experimental test

The compression tests of the systems were performed in the Experimental Structures Laboratory (LEE) of the University of Southern Santa Catarina (UNESC), located in the IParque-Scientific and Technological Park. A hydraulic cylinder with a load capacity of 50 tf of ENERPAC, a metal load applicator with dimensions of 18 × 10 cm, and Catman Easy software for data collection were employed for the test.

The raised floor systems were mounted on a naval plywood sheet on which the pedestal bases were screwed. To simulate the interlocking of the raised floor system, metal bars and plates were used for horizontal locking of the sides of the panels, which were fixed to the gantry supporting the hydraulic cylinder through washers.

The extent of the load applied to the systems was determined by the visual evaluation of the cracks in the ceramic tiles, and the breaking load was applied when a visible crack appeared. Figure 5 shows the experimental setup on the systems, where Figure 5(a) presents the application of load in the center of a ceramic tile; Figure 5(b) shows the bar and metallic plate blocking the system; and Figure 5(c) shows the application in the extremities of the four ceramic tiles.

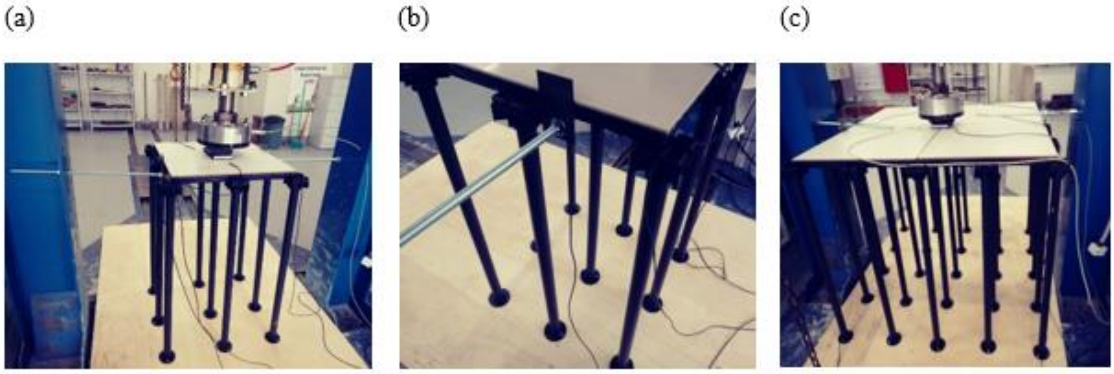

Figure 5: Mechanical test on 120 cm pedestals: (a) load application in the center of a ceramic plate, (b) bar and metal plate blocking the system, (c) load application at the ends of four ceramic tiles

3. Results and Discussion

A body fracture is defined as a segmentation into two or more parts under an applied load. This fracture can be ductile or brittle; a ductile fracture has a plastic deformation with intense energy absorption, and a brittle fracture occurs with limited or no plastic deformation (Zanotto and Migliore JR 1991).

In this study, the loads at which the systems failed were obtained by evaluating the deformations of the ceramic tiles. The load versus deformation curves of the systems indicated points where the deformations were accentuated, that is, points that express the loss of linearity of the curve. Based on this analysis, the collapse of the system was attributed to the loss of linearity in the strain curve as a function of the applied load. Thus, the load considered as a system collapse was the absolute value of the load at the same instant that the strain gauge readings indicated discontinuity in the curve.

Figure 6 presents the graphs containing the load versus deformation curves of the S-PT system in the adopted instrumentation positions. Figure 6(a), Figure 6(b), Figure 6(c) and Figure 6(d) present Position 1, Position 2, Position 3, and Position 4, respectively.

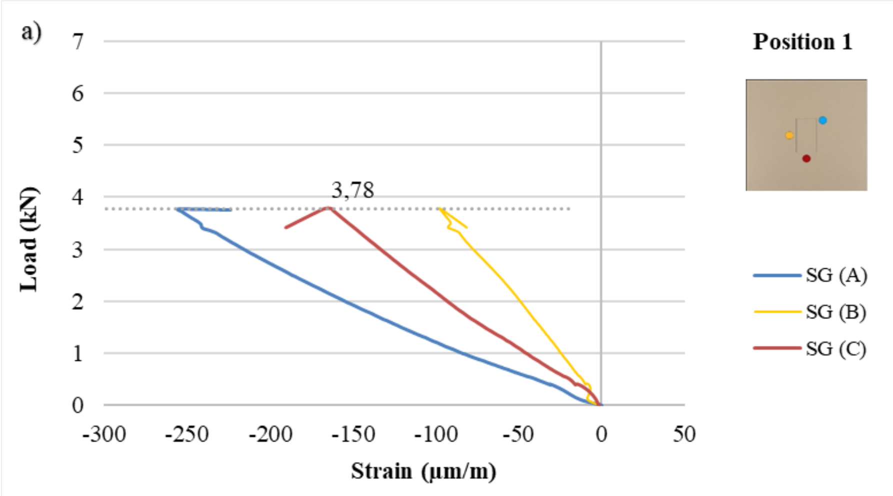

Figure 6(a): S-PT load versus strain graphs: (a) Position 1

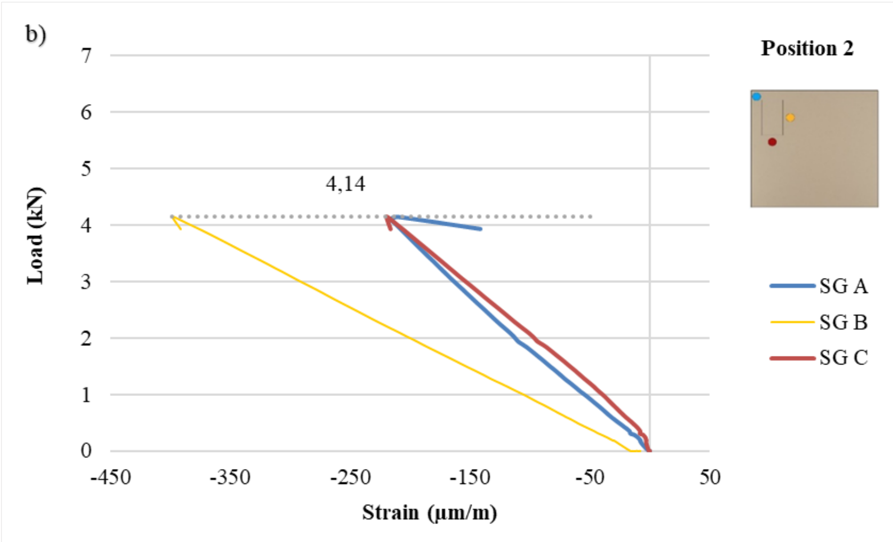

Figure 6(b): S-PT load versus strain graphs: (b) Position 2

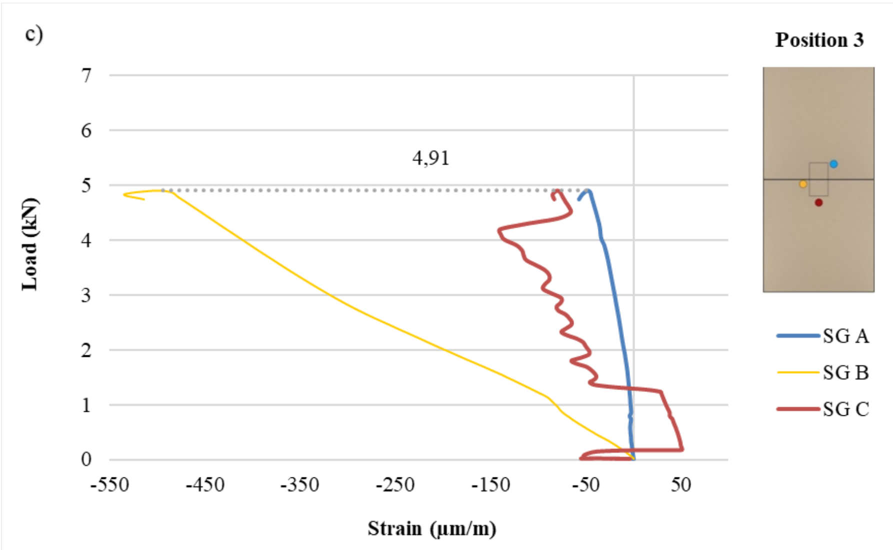

Figure 6(c): S-PT load versus strain graphs: (c) Position 3

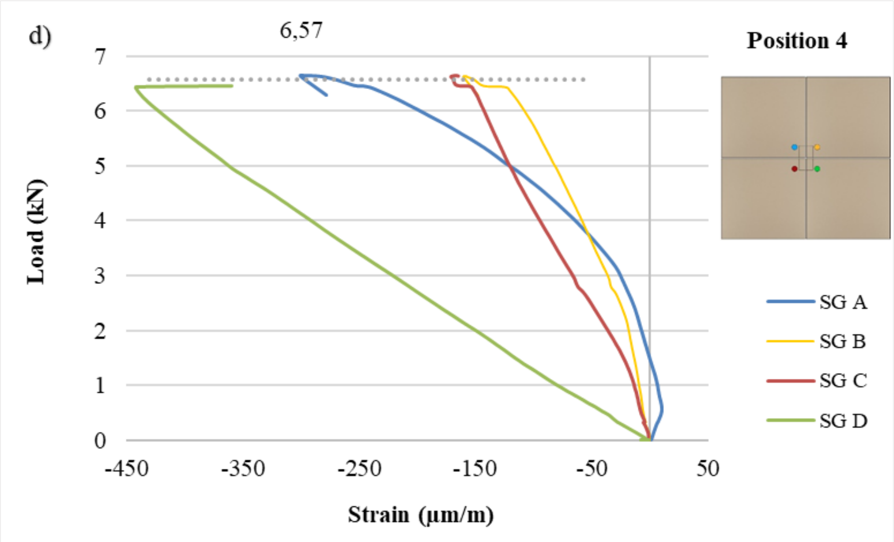

Figure 6(d): S-PT load versus strain graphs: (d) Position 4

It was observed through the analysis of the graphs in Figure 6 that in Position 1 of the S-PT system, the load versus strain curves had an abrupt linearity loss of approximately 3,78 kN, which was the breaking load of the system in this position. For Positions 2 and 4, the behavior of the curves was analogous to that of Position 1. The breaking loads were approximately 4,14 kN at Position 2 and 6,57 kN at Position 4.

At Position 3, strain gauges A and B reported curve amplitudes of approximately 4,91 kN. However, strain gauge C manifested irregular behavior, which was inconsistent with the other load versus strain curves evaluated in this study. This condition can be justified by the insufficient bonding of the strain gauge on the ceramic tile surface, which made it difficult to measure the actual strain.

By studying the load versus strain curves of the S-PE60 system, a simultaneous loss of linearity can be observed at the points where the moment of rupture was assigned, except for the curve obtained by strain gauge A at Position 2.

The graphs of load versus strain of the S-PE60 system are illustrated in Figure 7. Figure 7(a), Figure 7(b), Figure 7(c) and Figure 7(d) show the graphs for Positions 1, 2, 3, and 4, respectively.

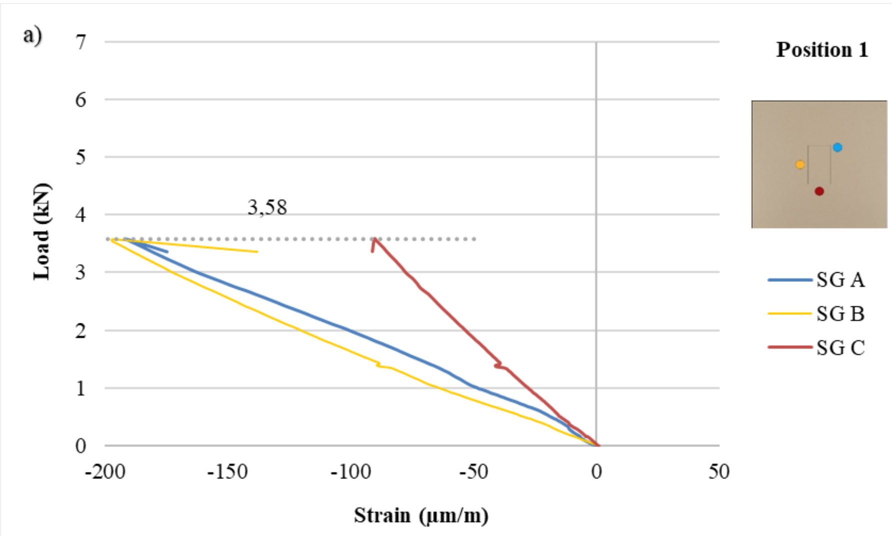

Figure 7(a): S-PE60 load versus strain graphs: (a) Position 1

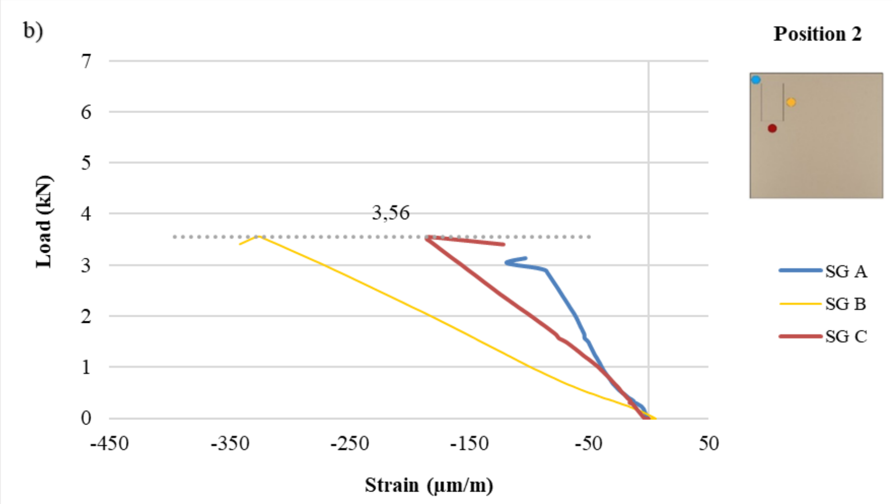

Figure 7(b): S-PE60 load versus strain graphs: (b) Position 2

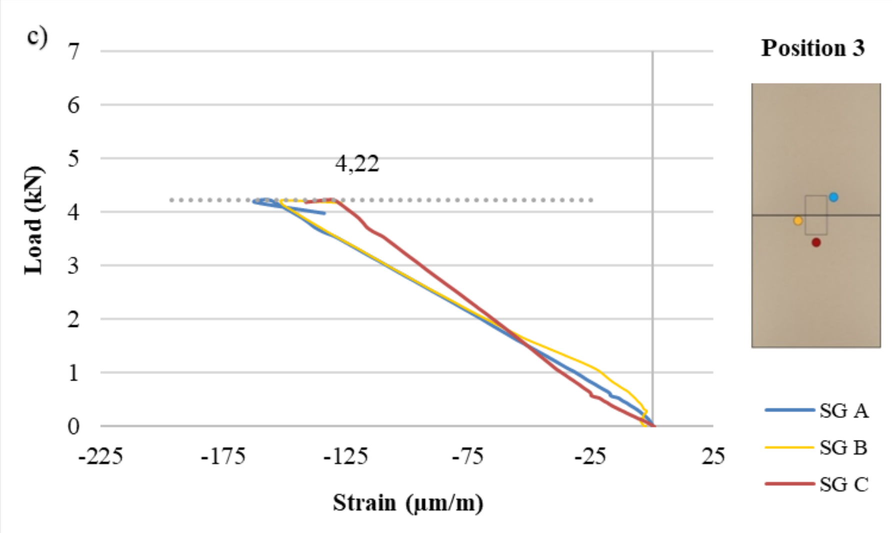

Figure 7(c): S-PE60 load versus strain graphs: (c) Position 3

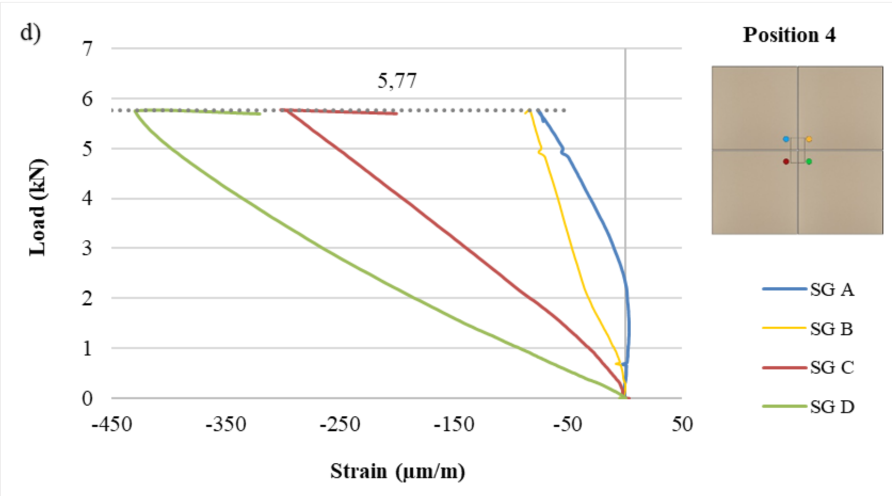

Figure 7(d): S-PE60 load versus strain graphs: (d) Position 4

For Position 1 of the S-PE60 system, the breaking load was approximately 3,58 kN. For Positions 3 and 4, the rupture loads were 4,22 kN and 5,77 kN, respectively.

As mentioned, the strain reading of strain gauge A at Position 2 was unique in relation to those of strain gauges B and C. The loss of linearity in the load versus strain curve of strain gauge A was approximately at 2,90 kN, whereas the curves obtained from strain gauges B and C indicated a rupture at 3,56 kN. This is because, according to Menegazzo et al. (2002) and Sesma (2014), ceramic materials have defects in their microstructure that can act as stress concentrators and starting points of rupture, reducing the load required for the rupture of the material.

In Figure 8, the graphs express the deformations for the S-PE120 system, where Figure 8(a), Figure 8(b), Figure 8(c), Figure 8(d), and Figure 8(e) show the deformations for Positions 1.1, 1.2, 2, 3.1, and 3.2, respectively.

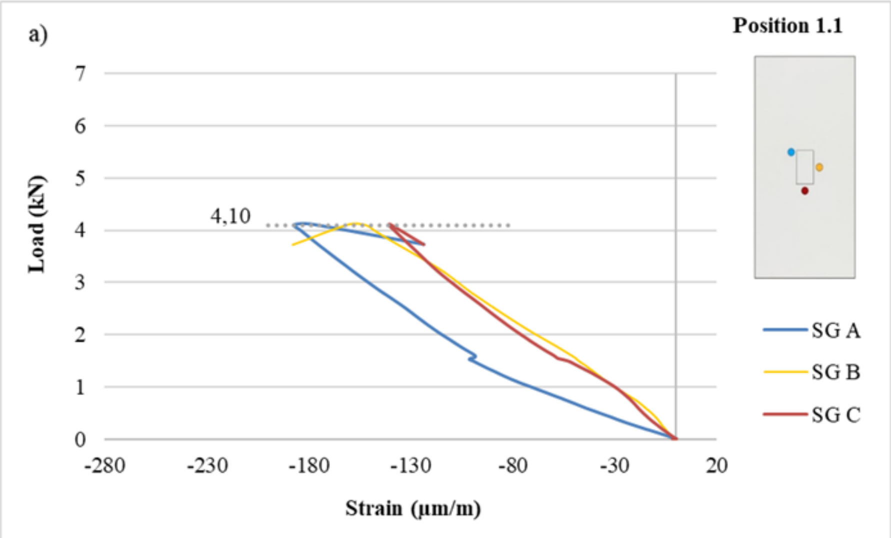

Figure 8(a): S-PE120 load versus strain graphs: (a) Position 1.1,

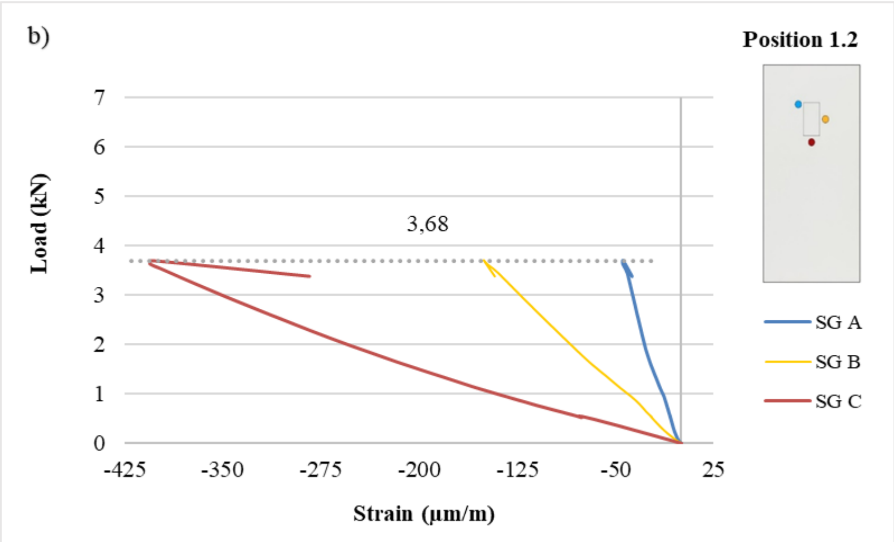

Figure 8(b): S-PE120 load versus strain graphs: (b) Position 1.2

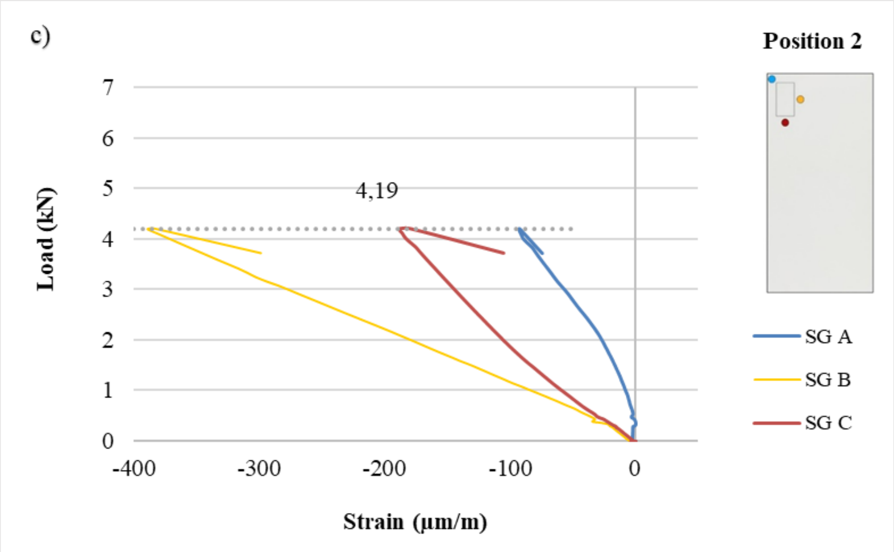

Figure 8(c): S-PE120 load versus strain graphs: (c) Position 2

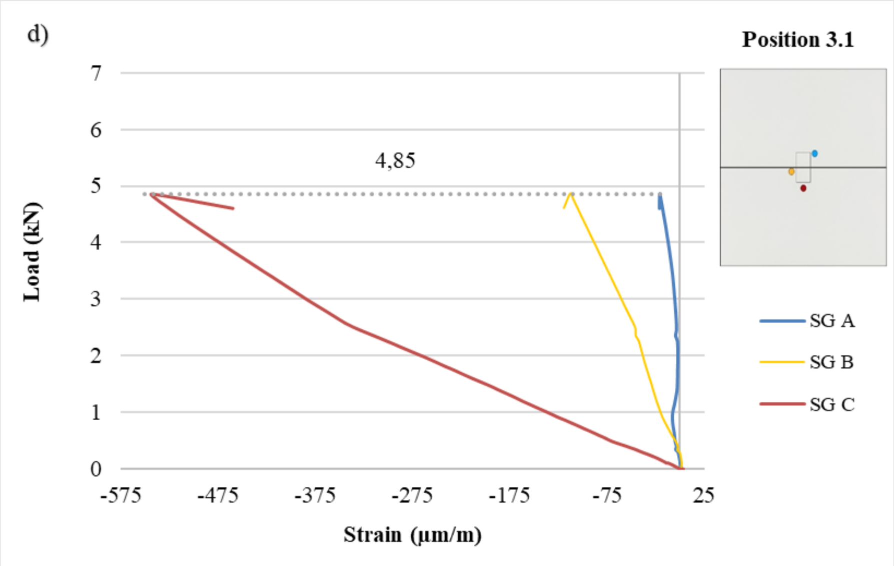

Figure 8(d): S-PE120 load versus strain graphs: (d) Position 3.1

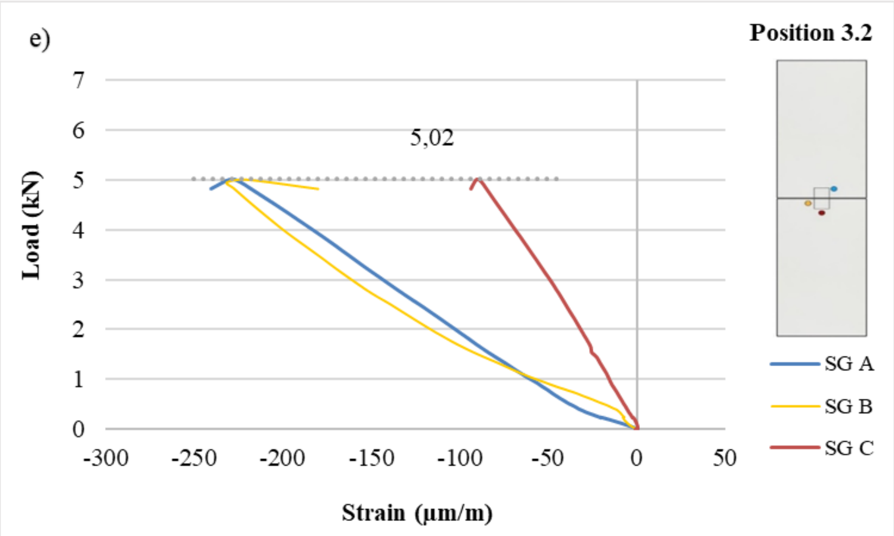

Figure 8(e): S-PE120 load versus strain graphs: (e) Position 3.2

The S-PE120 system at Positions 1.1, 1.2, 2, 3.1, and 3.2 had breaking loads of 4,10, 3,68, 4,19, 4,85, and 5,02 kN, respectively. In the load versus deformation curves of the S-PE120 system, a behavior similar to that of the two previous systems was observed. When the load applicator was positioned on a system composed of a single ceramic tile, the value of the breaking load was lower than that for systems composed of two or more ceramic tiles.

Figure 9 demonstrates the verified breaking loads for the S-PT, S-PE60, and S-PE120 systems ordered by the instrumentation positions. Figure 9(a) shows the breaking loads for the S-PT and S-PE60 systems, and Figure 9(b) shows the loads for the S-PE120 system.

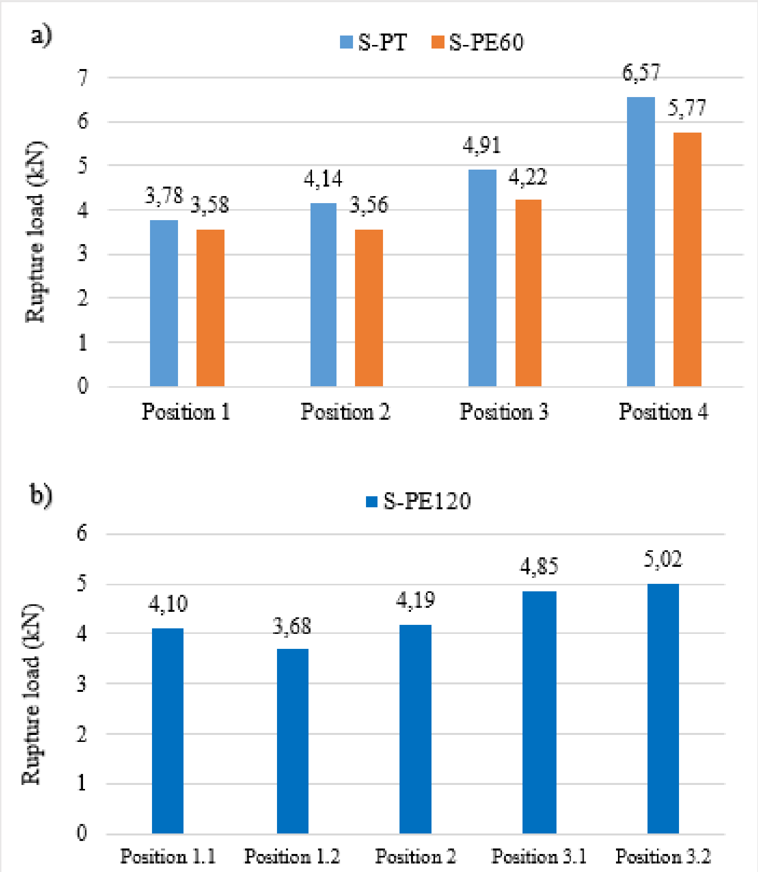

Figure 9: Systems rupture load

During the mechanical tests, when the load was applied to the systems, the edges of the plates opposite to the applicator experienced a vertical displacement. This displacement occurred because of the detachment of the plates near the pedestals. This condition provided relief and better distribution of stresses on the extension of the tiles as the structure did not remain fixed during the load application. That is, there was a freedom of displacement without adding deformation to the system. Therefore, higher breaking loads were achieved in the systems with more than one ceramic tile compared with those with a single ceramic tile.

Similarly, Positions 1 and 2 of the S-PT and S-PE60 systems presented lower breaking loads than those for Positions 3 and 4, and the breaking loads for Positions 1.1, 1.2, and 2 of the S-PE120 system were lower than those for Positions 3.1 and 3.2.

It was also verified that the rupture load was proportional to the number of ceramic tiles in the system. When the number of ceramic tiles in the system increased, the rupture load increased because additional spacing joints allowed further displacements in the system. Consequently, stress relief was achieved.

The failure loads, although close, at all positions were higher in the S-PT system than that in the S-PE60 system. This difference may be because the PT plate absorbs only 0.1% of the water, whereas the PE60 plate absorbs 0.5%. This property is intrinsically related to the bending strength of the material. The mechanical strength of a ceramic tile is associated with its water absorption capacity, which in turn, is related to the porosity of the tile. The more compact the material, the lower its porosity and, consequently, the lower its water absorption (Lima 1997; Rebelo 2010).

The results are also consistent with the breaking load values presented in Table 1. The water absorption and flexural strength properties of the S-PE group were similar. The difference between S-PE60 and S-PE120 is in the thickness of the piece, which gives a higher breaking load result for thicker pieces. This characteristic of the ceramic tile influenced the breaking load of the system, as shown in Figure 9. Comparing the systems with similar ceramic pieces—S-PE60 and S-PE120—for similar load application positions, a higher breaking load was observed for the S-PE120 system, which is consistent with the higher breaking load of its ceramic tile.

The strains measured by the strain gauges at the moment of rupture of the systems were all negative, which corresponded to the compression of the strain gauge. The compression of the strain gauges was due to the bending of the plates during the load application. The strain values do not exhibit uniformity in response to the applied loads. This variability occurs because ceramic tiles do not experience stress through plastic deformation (Medeiro 2018).

4. Conclusions

In this study, it was found that the positioning of the load applicator influences the rupture value, and the application of two or more ceramic tiles results in a high rupture value.

Furthermore, the systems with slabs having low water absorption exhibit high breaking loads. In the evaluation of slabs with the same absorption capabilities, the system with thick plates exhibits the best performance, indicating that the breaking load of the plate increases with thickness. This can be considered a determining factor for outdoor applications.

The integrity of the raised floor is compromised when one of its components is damaged. Hence, analyzing the strain is a plausible and effective methodology for evaluating the rupture load caused by ceramic tile failure.

The spacing between the tiles, called the joint, causes stress relief and allows greater deformations of the ceramic tiles, promoting resistance to high intensities of loads on the systems. Thus, the joints had a significant impact on the obtained results.

References

ABNT. 2014. *Projeto de Estruturas de Concreto - Procedimento*. ABNT NBR 6118:2014. Rio de Janeiro, Brazil: Associação Brasileira de Normas Técnicas.

de Albuquerque, M. da C. F., and J. de A. Rodrigues. 2006. "Characteristics of the double-torsion test to determine the R-curve of ceramic materials". *Materials Research* 9, no. 4: 361-68. https://doi.org/10.1590/s1516-14392006000400004.

Amorim, F. do C. 2015. "Influência da temperatura no comportamento mecânico do polímero Dgeba (Diglicidil Éter Bisfenol A)". Master's thesis, Mechanical Engineering, Fluminense Federal University.

Bernardes, M. 2009. "Tecnologia construtiva de piso elevado para áreas externas de edifícios". Master's thesis, Urban and Civil Construction Engineering, University of São Paulo. https://doi.org/10.11606/D.3.2009.tde-10032010-153812.

Caccia, C. S. 2012. "Placas cerâmicas para revestimento: Planilha eletrônica para auxílio na especificação". Undergraduate Courses, Civil Engineering, Federal University of Rio Grande do Sul. https://lume.ufrgs.br/handle/10183/63195.

Fonseca, E. S., F. G. Tavares, T. N. R. Sousa, and W. A. Morais. 2015. "Associação entre a morfologia de trincas de pisos cerâmicos e seu comportamento mecânico em fratura". *Ceramica* 61, no. 359: 303-08. https://doi.org/10.1590/0366-69132015613591915.

Kinzel, K. 2015. "Medidas de controle de escoamento na fonte: Estudo de caso de reservação sob piso elevado". Undergraduate Courses, Civil Engineering, Federal University of Rio Grande do Sul. https://hdl.handle.net/10183/127701.

Lima, L. C. 1997. "Materiais cerâmicos para revestimento: Considerações sobre produção e especificação". Master's thesis, São Carlos School of Engineering, University of São Paulo. https://repositorio.usp.br/item/000934312.

Medeiro, J. 2018. "Sistemas de piso com revestimento cerâmico: avaliação da resistência a cargas verticais concentradas". Undergraduate Courses, Civil Engineering, University of the Extreme South of Santa Catarina. http://repositorio.unesc.net/handle/1/6508.

Menegazzo, A. P. M., J. O. A. Paschoal, A. M. Andrade, J. C. Carvalho, and D. Gouvêa. 2002. "Avaliação da resistência mecânica e módulo de Weibull de produtos tipo grês porcelanato e granito". *Cerâmica Industrial* 7, no. 1: 24-32.

Morais, A. M. R., C. Santos, M. Rodrigues, and V. L. Igel. 2017. "Construção de um edifício comercial sustentável: Estudo de caso Em Atibaia". Civil Engineering, Faculdades Atibaia-Faat.

Moreiras, S. T. F. 2014. "Metodologias para o dimensionamento de placas de "granitos" em sistemas não-aderentes de fixação". PhD diss., São Carlos School of Engineering, University of São Paulo. https://doi.org/10.11606/T.18.2014.tde-29052014-150736.

Moritz, R. B. 2018. "Estudo comparativo entre as tecnologias construtivas de pré-laje e piso elevado em áreas externas: Estudo de caso em empreendimento de edificações misto". Undergraduate Courses, Civil Engineering, Federal University of Rio de Janeiro.

Rebelo, C. da R. 2010. "Projeto e execução de revestimento cerâmico - interno: interno". Graduate Courses, Especialização em Construção Civil, Universidade Federal de Minas Gerais. https://hdl.handle.net/1843/BUOS-9AAH5D.

Sesma, N. M. 2014. "Estudo das propriedades de uma cerâmica vermelha sinterizada em diferentes temperaturas". Undergraduate Courses, Civil Engineering, Engineering School of Lorena, University of São Paulo.

Zanotto, E. D., and A. R. Migliore JR. 1991. "Propriedades mecânicas de materiais cerâmicos: Uma introdução". *Ceramica* 37: 7-16.

Zhang, G., J. Yang, and A. C. Sidwell. 2002. "- Raised floor system: A paradigm of future office building fitout?". In *Advances in Building Technology*, edited by M. Anson, J. M. Ko, and E. S. S. Lam, 1577-84. Oxford: Elsevier. https://doi.org/10.1016/B978-008044100-9/50195-9.

Acknowledgments

We would like to thank Editage (www.editage.com) for English language editing.

Financial support

This work collaborated with Eliane Revestimentos Cerâmicos in acquiring the ceramic tiles used in the tests.